International Journal of GEOMATE, Dec., 2023 Vol.25, Issue 112, pp.107-114
ISSN: 2186-2982 (P), 2186-2990 (O), Japan, DOI: https://doi.org/10.21660/2023.112.g13370
Geotechnique, Construction Materials and Environment

NEURAL NETWORK APPLICATION FOR FINE-BLANKED EDGE QUALITY IN ROLLED STEEL SHEETS

Thanyaphon Nakkhlai[1,2], Watcharapong Chookaew[1], Juthanee Phromjan[1,2], Chakrit Suvanjumrat[1,2,*] and Ravivat Rugsaj[3]

[1]Department of Mechanical Engineering, Faculty of Engineering, Mahidol University, Salaya, Nakhon Pathom 73170, Thailand;
[2]Laboratory of Computer Mechanics for Design (LCMD), Department of Mechanical Engineering, Faculty of Engineering, Mahidol University, Salaya, Nakhon Pathom 73170, Thailand;
[3]Department of Mechatronics Engineering and Artificial Intelligence, Vincent Mary School of Engineering, Assumption University, Samut Prakan 10570, Thailand

*Corresponding Author, Received: 09 June 2023, Revised: 27 Nov. 2023, Accepted: 28 Nov. 2023

ABSTRACT: The backing plate plays a crucial role in drum brakes, pushing the brake shoe against the drum for effective vehicle braking and road safety. Manufactured from steel sheets, it exhibits properties akin to a composite material, with characteristics varying based on directionality. The backing plate's profile features a continuous series of arcs, making the fine-blanked edge quality contingent on the arc radius. This research delved into fine-blanked manufacturing through a combination of experimentation and simulation to discern the impact of the arc radius on edge quality. Employing a scanning electron microscope for edge quality investigation and benchmarking the finite element model against it, the study ensured a comprehensive understanding. The well-aligned finite element model served as input data for training an artificial neural network (ANN), specifically engineered to accurately estimate backing plate edge quality. This ANN is anticipated to be instrumental in designing future steel plate profiles boasting multiple arcs, offering precision in the manufacturing process for enhanced edge quality.

Keywords: Artificial Neural Network, Backing plate, Drum brake, Edge quality, Finite element method

1. INTRODUCTION

The backing plate stands out as a vital element within a drum brake, serving as the robust foundation for this braking system. Crafted from carbon steel, the manufacturing process relies on conventional fine blanking to intricately cut the backing plate from a rolled steel sheet. This procedure holds substantial significance in the automotive industry. In this process, the rolled steel sheet undergoes drawing into the cutting machine equipped with essential components like a punch, die, and blank holder—integral parts of the cutting tool. As the plate assumes the cutting position, the blank holder and punch consecutively impact the plate with the desired velocity. Consequently, the backing plate takes its final shape in preparation for the subsequent deep drawing process [1].

As previously mentioned, distinct areas emerge along the edge of the backing plate as a result of the fine blanking process, encompassing rollover, shear, fracture, and burr zones. The quality of the edge is directly influenced by these zones, with optimal results observed when the ratio between fracture and plate thickness approaches zero [2]. A high-quality edge is achieved when there is a predominant shear zone. The characterization of these zones is typically conducted through the use of a scanning electron microscope (SEM). In instances where a defective edge is identified, resorting to the grinding method becomes necessary in the production process. Unfortunately, this introduces complications and inefficiencies in the manufacturing of the backing plate.

The emergence of different zones on the cutting edge is attributed to a multitude of factors. Huang et al. [3] conducted a study on the fine blanking process involving various metals and metal thicknesses. They introduced an annular trough at a die to enhance the quality of the shear zone. Another study by Zheng et al. [4] focused on analyzing the sheared surface quality by subjecting stainless steel plates to different temperatures. They observed that a temperature increase up to 250°C could complete the shear zone. Investigating edge quality is both time-consuming and costly, leading to the adoption of the finite element method (FEM) as a high-end computational technique for simulating the fine blanking process [5-8]. Canales et al. [9] utilized the Metafor software based on FEM to simulate the blanking process, validating their results against experimental data. Mao et al. [10] employed 2D FEM to examine fine blanking sprockets, revealing insights into rollover formation and providing color-contoured depictions of temperature, strain, and velocity fields during the process. Xincun et al. [11] explored the effect of blanking clearance using FEM, discovering that increased clearance accelerated damage accumulation, causing an early material fracture in the shear zone. FEM with the Lemaitre damage model accurately modeled fine blanking; shear surface and burr height matched experimental results [12]. Li et al. [13] simulated the hot blanking process of boron steel, employing various fracture criteria and finding that Oyane and Brozzo criteria aligned well with experimental results. Liu et al. [14] used FEM to reduce die-roll size in the fine blanking process by modifying the die structure, while He et al. [15] optimized the clearance range in blanking processes through FEM, determining an optimal clearance for non-oriented electrical steel sheets. Sahli et al. [16] observed that a reduction in clearance could delay fracture initiation, with FEM simulation results aligning with experimental data.

The fine blanking process modeling can be quite time-consuming when using the FEM. Calculating optimum values for each modeling task within the fine blanking process also takes a considerable amount of time. To address this, researchers have explored the application of Artificial Neural Networks (ANN) as an alternative method to reduce modeling time for simulation and optimization compared to FEM. Hambi [17] and Hambi and Guerin [18] developed an ANN to predict the height of the burr on the cutting zones' edges, with the input variable being the distance between the punch and the die. In a study by Al-Momani et al. [19], a comparison between Multiple Regression Analysis (MRA) and ANN revealed that the ANN outperformed MRA in accuracy when determining the height of burrs on workpieces. This underscores the potential of ANN to offer faster and more precise predictions in the context of fine-blanking processes.

2. RESEARCH SIGNIFICANCE

The backing plate profile, defined by a continuous series of arcs, is pivotal in determining edge quality. This research focuses on modeling the fine blanking process for drum brake backing plates, investigating the impact of arc radius on edge quality. Simulation results will be rigorously compared with experimental data to establish the arc radius-edge quality relationship. This insight will inform the design of backing plate profiles. The study also explores using the ANN method to predict Finite Element Analysis (FEA) results, offering the potential for estimating the edge quality of backing plates with multiple arcs in future applications.

3. EXPERIMENTS

Two distinct methodologies were employed to scrutinize the edge quality of the backing plate. The first involved material testing, where meticulous attention was given to ascertaining the mechanical properties of the backing plate material. Concurrently, a fine blanking test was conducted to assess and characterize the edge quality of the backing plates. This involved a detailed examination of various zones on the edge surfaces, with measurements and investigations carried out to gain insights into the characteristics of each zone. The combination of material testing and fine blanking tests provides a comprehensive understanding of the backing plate's edge quality, allowing for a thorough analysis and interpretation of the results.

3.1 Backing Plate Property

Backing plates are crafted from a rolled steel sheet with a thickness of 6.00 mm and a width of 256.00 mm. The steel-coil feeding and blanking machines are utilized to draw the steel plate, and subsequently, the steel sheet is cut into tensile specimens in both longitudinal and transverse directions using laser cutting techniques. These specimens, designed in accordance with ASTM E8/04 specifications (Fig. 1), are subjected to tension testing using a universal testing machine (Instron 5969) following ASTM E8/04 standards. The true stress vs. true strain graph from the tensile testing is depicted in Fig. 2. Notably, the specimens in the longitudinal direction exhibit elastic properties up to a strain of 0.006, with a measured tensile strength of 232.85 MPa, and the breaking point occurring at a true strain of 0.25. These

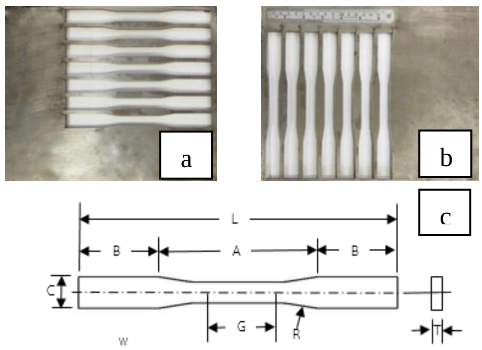

Fig. 1 Specimens by the laser cutting technique in (a) longitudinal length (b) transverse length, and (c) their detail according to ASTM E8/04

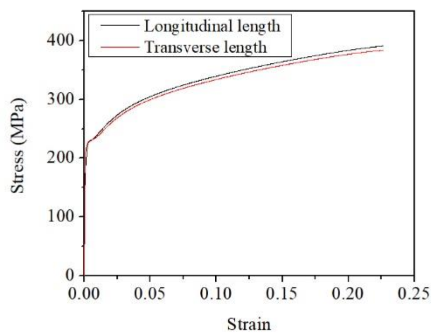

Fig. 2 Stress vs. strain graphs of specimens

findings indicate that the tensile properties of the backing plate in both directions are closely aligned, supporting the characterization of the backing plate as possessing isotropic material properties.

3.2 Fine Blanking Process of Backing Plates

The fine blanking process was conducted using the Seyi blanking machine (SM1-300). A strengthener was employed to flatten a rolled sheet, facilitating the integration of three blanking steps to form the backing plate. This blanking machine executed the punching and die-cutting of two holes within the backing plate and its profile. Figure 3 provides a visual representation of the blanking machine, showcasing three punches and three dies essential for the production of the backing plate. Throughout the fine blanking test, the punch impacted the flattened plate at a velocity of 0.18 m/s, maintaining a clearance of 0.6 mm between the punch and die. Figure 4 illustrates the resulting blanking workpiece of the backing plate. To scrutinize and measure the zones on the edge surface of the blanking workpiece, scanning electron and transmission electron microscopes (SEM) were employed.

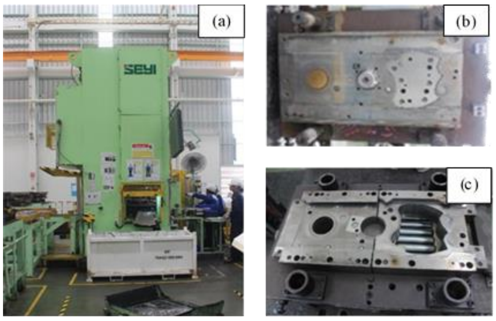

Fig. 3 (a) The blanking machine, (b) punches, and (c) dies for the fine blanking process of the backing plate

Fig. 4 The sample of the backing plate

3.3 Fine Blanking Process Modeling

The fine blanking process underwent modeling using MSC Dytran software, employing FEM. Shell elements were used for all parts except the workpiece, which required a solid model due to the need to investigate edge quality. In this context, the flattened plate with two holes was created using solid elements to ensure accuracy in assessing edge characteristics. Figure 5 illustrates the arrangement of the finite element model for the fine blanking process, specifically in the final step of producing the backing plate. The plate model consisted of a combination of hexahedron and tetrahedron elements, progressively stacked to match the total thickness of the rolled steel sheet. With over twenty layers, these hexahedron elements were sized at less than 0.3 mm. Additionally, fine elements were strategically placed along the profile of the backing plate. For detailed reference, the finite element model of each component in the fine blanking process is outlined in Table 1.

The workpiece in the fine blanking process was characterized by an elastic-plastic function to regulate the deformation and fracture of the backing plate material. Specifically, in the plastic deformation range, experimental data was incorporated into the stress-strain table of the material function. This approach ensured that the deformable behavior of the workpiece was closely aligned with the material properties observed during tensile testing. The termination of the workpiece was determined by assigning the failure strain to the material function. In contrast, other components in the fine blanking process, such as the punch, die, and blank holder, were modeled using a rigid material model. Given their resistance to deformation, these components were considered challenging to deform, particularly in scenarios involving contact-impact phenomena. This comprehensive modeling strategy aimed to capture the intricate interplay of material behavior and mechanical interactions within the fine blanking process.

In the fine blanking simulation, the punch model descended with a vertical velocity of 0.18 m/s, replicating the experimental conditions. Simultaneously, the blank holder moved at the same

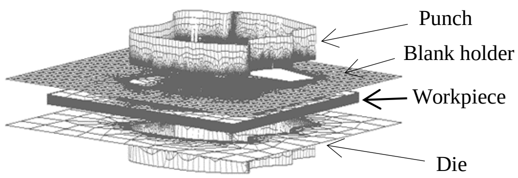

(a)

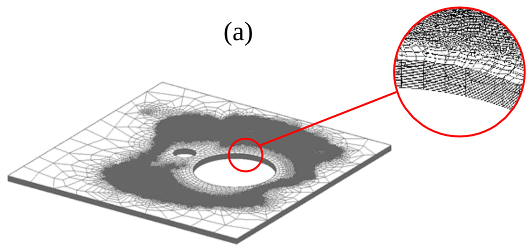

(b)

Fig. 5 Finite element model of (a) the fine blanking parts and (b) the workpiece

Table 1 Element properties of the fine blanking components

Part	Element type	Element	Node
Punch	Shell	11,093	11,952
Blank holder	Shell	2,319	2,747
Workpiece	Solid	1,533,660	1,611,477
Die	Shell	6,431	6,499

speed to secure the workpiece during its interaction with the descending punch. The workpiece, positioned on the die, was set as fixed. The dynamic interaction between the punch and the workpiece, facilitated by the contact-impact algorithm, utilized a master-slave contact approach [20]. Notably, this algorithm managed the collision and interaction between the punch and blank holder with the deformable workpiece. All finite element models were executed on a personal computer equipped with a Core i7 CPU and 4GB RAM, ensuring computational efficiency throughout the simulation process.

3.4 Artificial Neural Network

In the assessment of the fine blanking process for the drum brake backing plate, the quality of the edges was evaluated using an Artificial Neural Network (ANN). Training data for the ANN were derived from FEA, with inputs comprising the radius of the workpiece curves, punch velocities, and the clearance between the punch and die. The corresponding outputs included the thickness values for the rollover, shear, and fracture zones. The architecture of the ANN incorporated two hidden layers. Multiple input neurons, along with the two hidden layers, were trained to grasp the intricacies of the fine blanking process. The log-sigmoid transfer function was applied in the first hidden layer, while the second hidden layer utilized the linear transfer function. The first hidden layer consisted of 5 neurons, and the second hidden layer had 3 neurons. Figure 6 illustrates the structure of the ANN designed for modeling the fine blanking process of the backing plate.

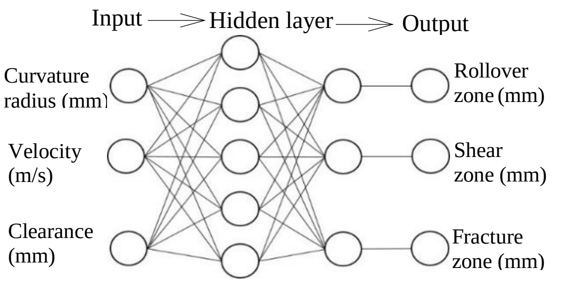

Fig. 6 Artificial neural network structure of the fine blanking process

4. RESULTS AND DISCUSSION

4.1 Validation of Cutting Zones

During the analysis of the fine blanking model, the strain experienced by the workpiece from various fine blanking components was visualized using color contours in the FEM. The color spectrum ranged from red, indicating maximum strain, to blue, representing minimum strain. Figure 7 presents the evolution of strain on the workpiece from the initial stages of the process to the final product. The backing plate model illustrated strain along its edge. Moreover, the FEM depicted the cutting action on the workpiece's edge by the punch and die (Fig. 8). Elements at the workpiece's top were influenced by the punch during its impact with the die, resulting in a rounded edge known as the rollover zone. Subsequently, the collapsing of elements caused by the punch and die created the shear zone on the backing plate's edge.

In this period of the fine blanking process, the shear zone formed as elements along the edge profile reached the failure strain value and separated. The finite element model effectively captured the distinct rough surface characteristics of different zones, allowing for a detailed investigation into the deformation and fracture of elements. The distance between these zones was quantified and digitized by classifying changing elements. To validate the thickness of zones on the backing plate model's edge, the SEM images were used as a reference, ensuring accuracy in the representation of fine blanking-induced deformations and fractures.

Figure 9 provides a comparison between the SEM image and the FEA result at the largest radius (48.5 mm) of the edge profile of the backing plate. The SEM image is magnified with a scale of 1:500 mm, projected normally to the edge of the backing plate. Three distinct zones were identified: the rollover zone at the top of the edge surface, the shear zone in the middle, and the fracture zone at the bottom. Each zone exhibited characteristic features. The rollover zone manifested as a rounded corner on the edge, the shear zone was observable at the splintered area on the edge surface, and the fracture zone constituted the remaining rough edge surface.

Remarkably, the characteristics of each zone observed in the SEM image aligned with the features predicted by the FEA results. The rollover, shear, and fracture zones identified in the FEA corresponded well with the SEM findings. This agreement between the simulation and experimental results underscored the effectiveness of the Finite Element Analysis in accurately capturing the deformations and failures induced by the fine blanking process on the edge of the backing plate.

In Figure 10, a comprehensive comparison between each zone from the finite element model and the experimental results is presented. The

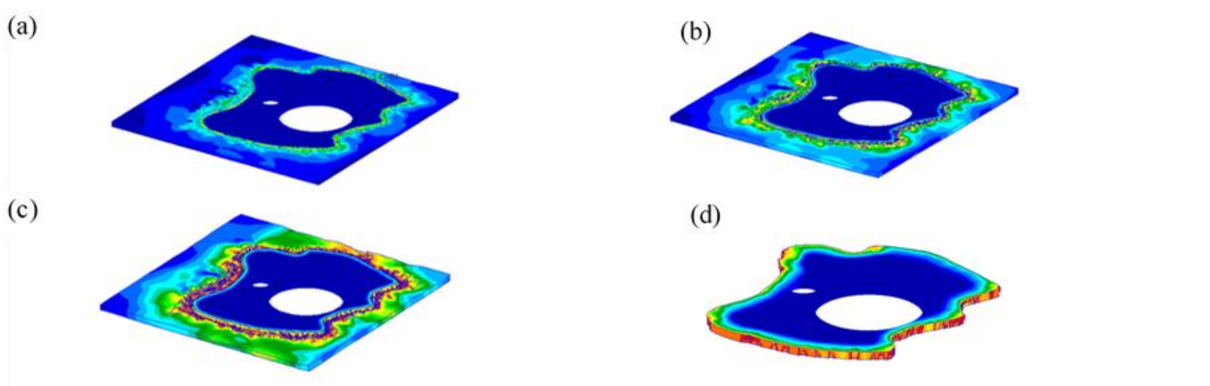

Fig. 7 The strain results on the workpiece at (a) t = 0.000003 sec, (b) t = 0.000004 sec, (c) t = 0.000005 sec, and (d) t = 0.000006 sec.

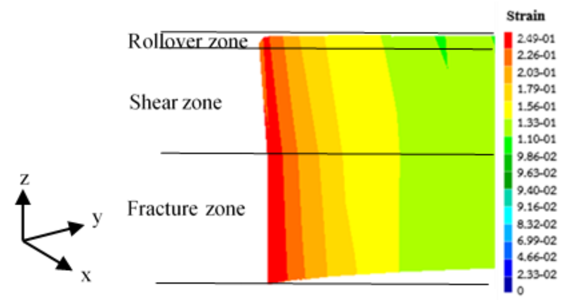

Fig. 8 Edge of the workpiece cutting off by the punch and die

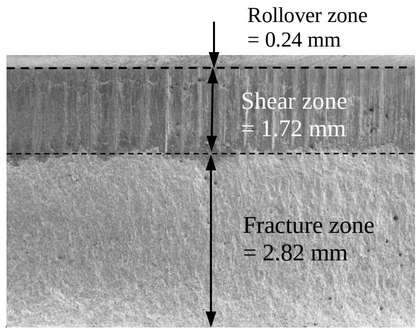

(a)

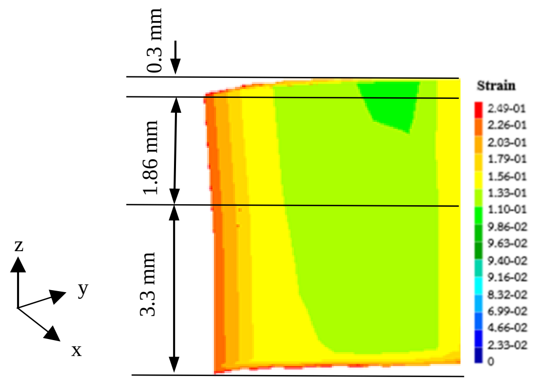

(b)

Fig. 9 SEM image (a) comparing the FEA result (b) at a radius of 48.5 mm on the edge profile

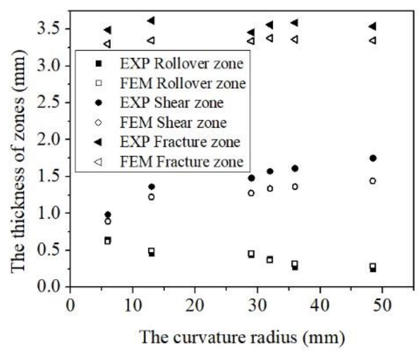

Fig. 10 Comparison of each zone between the FEM and experiment

simulation zones exhibited a strong agreement with the experimental observations. Specifically, the shear zone in the FEA results showed an average error of less than 17.71%, while the rollover and fracture zones demonstrated even smaller average errors, measuring less than 16.67% and 11.81%, respectively. This level of consistency between the simulated and experimental zones further validates the accuracy and reliability of the Finite Element Analysis in replicating the deformations and failures observed in the fine blanking process on the various zones of the backing plate's edge. The close alignment between simulation and experiment reinforces the utility of FEA as a predictive tool in understanding and optimizing the fine blanking process.

4.2 Radius Effects on Edge Quality

Figure 11 illustrates a comparison of the thickness of each zone along the edge profile, magnified by SEM at each curve of the edge profile. The analysis revealed that as the curvature radius increased, the rollover zone decreased, while the fracture zone also exhibited a decrease with an increasing curvature radius. The edge quality was assessed based on the quantity of shear zone thickness present on the edge surface. Notably, the edge of the backing plate exhibited the highest quality at a curvature radius of 48.5 mm, where the shear zone thickness accounted for more than 28.40% of the edge thickness.

This observation underscores the sensitivity of edge quality to the curvature radius, indicating that certain curvature radii contribute to superior edge characteristics, particularly with respect to the thickness of the shear zone. The insights gained from this analysis can be valuable for optimizing the fine blanking process and achieving desired edge qualities in the production of backing plates.

In Figure 12, correlation graphs depict the influence of the radius on the thickness of zones on the cutting edge. The thickness of the rollover, shear, and fracture zones varies with the curvature radius of the backing plate profile, as determined by Eqs. (1), (2), and (3), respectively. Notably, these equations provide a quantitative representation of the relationship between the curvature radius and the thickness of each zone. The correlation coefficients (R^2) associated with Eqs. (1), (2), and (3) are reported as 0.82, 0.86, and 0.02, respectively.

$$t_r = -0.0086r + 0.6376 \quad (1)$$
$$t_s = 0.0163r + 1.0122 \quad (2)$$
$$t_f = 0.0003r + 3.5363 \quad (3)$$

where t_r denotes the rollover zone thickness, t_s denotes the shear zone thickness, t_f denotes the fracture zone thickness, and r denotes the curvature radius.

These correlation coefficients reflect the degree of linear correlation between the curvature radius and the thickness of each zone. A higher R^2 value indicates a stronger correlation. In this case, the rollover and shear zones demonstrate moderate to strong correlations with the curvature radius, as evidenced by R^2 values of 0.82 and 0.86. On the other hand, the fracture zone exhibits a weaker correlation, as indicated by the lower R^2 value of 0.02. These correlations provide valuable insights into the quantitative relationships governing the impact of curvature radius on the thickness of different zones on the cutting edge during the fine blanking process.

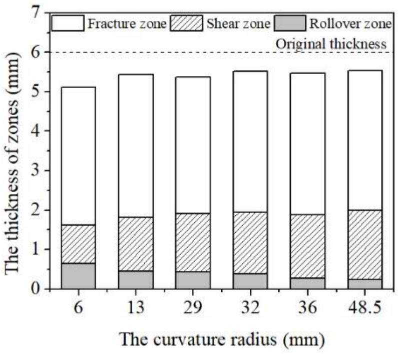

Fig. 11 Thickness of each zone at various radiuses along the edge profile, which is expanded by SEM

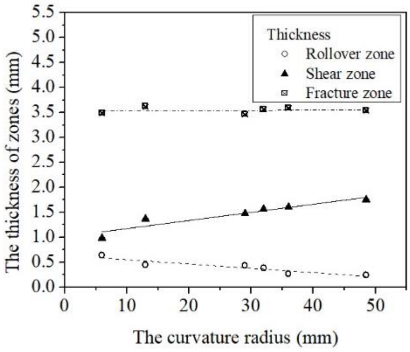

Fig. 12 Correlation graphs of radius effects on the thickness of each zone of the cutting edge

4.3 Artificial Neural Network Application

In MATLAB software, the ANN was trained for the estimation of edge quality. The input data consisted of 36 samples used for training and predicting the thickness of each zone along various curvature radii on the edge profile. Comparative results between the thickness of each zone on the edge at various curvature radii and punching speeds obtained by the ANN and the FEA are presented in Figure 13. The punching speeds examined were 0.01 m/s, 0.09 m/s, 0.18 m/s, and 0.27 m/s.

The comparison revealed that the thickness of each zone could be accurately predicted by the ANN, with an average error of 13.67% when compared to the FEA results. This strong agreement indicates that the ANN is a reliable tool for rapidly predicting the thickness of each zone along the edge profile. The ability of the ANN to closely replicate the FEA results suggests its potential utility in edge quality estimation, offering a more efficient alternative for certain predictive tasks in the context of the fine blanking process.

5. CONCLUSION

The backing plate, characterized by a complex shape with varying radius sizes along its edge, presents challenges in achieving consistent cutting zone thickness. The cutting zone, divided into rollover, shear, and fracture zones, demands particular attention to enhance edge quality, especially by reducing the thickness of the fracture zone. Experimental findings indicated that smaller radii resulted in lower-quality edges. While FEM proved effective in investigating and improving edge quality, its preparation and analysis were time-consuming, yielding an average error of 15.39% compared to experimental results.

To streamline the prediction of edge quality, an ANN was developed. The ANN structure featured

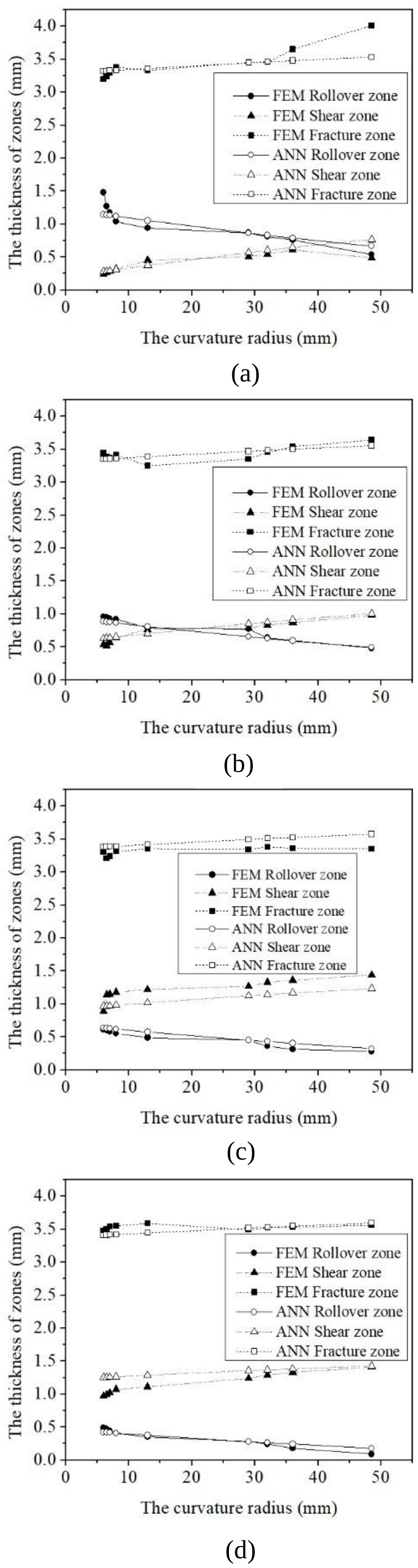

Fig. 13 Comparison of the thickness of each zone at various radiuses along the edge profile between the-ANN and the FEM at punch speed of (a) 0.01 m/s, (b) 0.09 m/s, (c) 0.18 m/s, and (d) 0.27 m/s

log-sigmoid and linear transfer functions, each with five and two neurons, respectively. Training the ANN required only 36 input data points to predict the thickness of cutting-edge zones rapidly. This ANN demonstrated a quick and accurate prediction, aligning well with FEA results. The integration of ANN and FEM holds promise for efficiently predicting edge quality, offering valuable insights for the design of steel plate profiles with intricate arc patterns in future applications.

6. ACKNOWLEDGMENTS

This research was made possible through financial support from the Thailand Research Fund (TRF) and Hosei Brake (Thailand) Co., Ltd under Research and Researchers for Industries (RRI) Grant No. MSD62I0067. We extend our gratitude for their support in advancing this work and contributing to the understanding and improvement of the fine blanking processes in the industry.

7. REFERENCES

[1] Zheng Q, Zhuang X., and Zhao Z., State of the art and future challenge in fine-blanking technology. Production Engineering, Vol. 13, 2018, pp. 61-70.

[2] Aravind U., Chakkingal U., and Venugopal P., A review of fine blanking: influence of die design and process parameters on edge quality. Journal of Materials Engineering and Performance, Vol. 30, 2020, pp. 1-32.

[3] Huang GM., Wang JP., Hsu MH., Huang KC., Chen TT., and Chen TC., Application of mold trough design to blanking technology. The International Journal of Advanced Manufacturing Technology, Vol. 88, 2017, pp. 1025-1034.

[4] Zheng Q., Zhuang X., Hu J., and Zhao Z., Formability of the heat-assisted fine-blanking process for 304 stainless steel plates. Materials Characterization, Vol. 166, 2020, pp. 110452.

[5] Phromjan J., and Suvanjumrat C., Non-pneumatic tire with curved isolated spokes for agricultural machinery in agricultural fields: Empirical and numerical study, Heliyon, Vol. 9, 2023, pp. e18984.

[6] Phromjan J., and Suvanjumrat C., Development of solid tire model for finite element analysis of compressive loading, Songklanakarin Journal of Science and Technology, Vol. 43, Issue 1, 2021, pp. 229-236.

[7] Phromjan J., and Suvanjumrat C., Effects on spoke structure of non-pneumatic tires by finite

element analysis, International Journal of Automotive Technology, Vol. 23, Issue 5, 2022, pp. 1437-1450.

[8] Rugsaj R., and Suvanjumrat C., Determination of material property for non-pneumatic tire spokes by inverse method. Key Engineering Materials, Vol. 777, 2018, pp. 411-415.

[9] Canales C., Bussetta P.,and Ponthot JP., On the numerical simulation of sheet metal blanking process. International Journal of Material Forming, Vol. 10, 2017, pp. 55-71.

[10] Mao H., Li S., Liu Y., and Hua L., An investigation on the microstructure of the fine-blanked sprocket. The International Journal of Advanced Manufacturing Technology, Vol. 90, 2017, pp. 3171-3185.

[11] Xincun Z., Siming M., and Zhen Z., A microstructure-based macro-micro multi-scale fine-blanking simulation of ferrite-cementite steels. International Journal of Mechanical Sciences, Vol. 128-129, 2017, pp. 414-427.

[12] Isik K., Yoshida Y., Chen L., Clausmeyer T., and Tekkaya AE., Modelling of the blanking process of high-carbon steel using Lemaitre damage model. Comptes Rendus Mécanique, Vol. 346, Issue 8, 2018, pp. 770-778.

[13] Li H., Hou H., Li Z., He L., and Wang X., Numerical simulation of hot blanking for boron steel B1500HS based on ductile fracture criterion. The International Journal of Advanced Manufacturing Technology, Vol. 97, 2018, pp. 3505-3522.

[14] Liu Y., Tang B., Hua L., and Mao H., Investigation of a novel modified die design for fine-blanking process to reduce the die-roll size. Procedia Engineering, Vol. 207, 2017, pp.1546-1551.

[15] He J., Wang Z., Li S., Dong L., Cao X., and Zhang W. Optimum clearance determination in blanking coarse-grained non-oriented electrical steel sheets: experiment and simulation. International Journal of Material Forming, Vol. 12, 2019, pp. 575-586.

[16] Shali M., Roizard X., Assoul M., Colas G., Gaimpiccolo S., and Barbe J. P., Finite element simulation and experimental investigation of the effect of clearance on the forming quality in the fine blanking process. Microsystem Technologies, Vol. 27, 2021, pp. 871-881.

[17] Humbli R., Prediction of burr height formation in blanking processes using neural network. International Journal of Mechanical Sciences, Vol. 44, 2002, pp. 2089-2102.

[18] Humbli R., and Guerin F., Application of neural network for optimum clearance prediction in sheet metal blanking processes. Finite Elements in Analysis and Design, Vol. 39, 2003, pp. 1039-1052.

[19] Al-Momani ES., Mayyas AT., Rawabdeh I., and Alqudah R., Modeling blanking process using multiple regression analysis and artificial neural networks. Journal of Materials Engineering and Performance, Vol. 21, 2012, pp. 1611-1619

[20] Suvanjumrat C., and Puttapitukporn T., Determination of drop-impact resistance of plastic bottles using computer aided engineering. Kasetsart Journal (Natural Science), Vol. 45, Issue 5, 2011, pp. 932-942.